Nonlinear Dynamics and Systems Theory, **16** (1) (2016) 20–34

Investigation in the Technique of Adaptive Predictive Control Fed by a Hybrid Inverter Applied to a Permanent Magnetic Synchronous Machine

I. Bentchikou [1], F. Boudjema [1], D. Boukhetala [1], A. Tlemçani [2*] and N. Ould Cherchali [2]

[1] *Laboratory of Process Control, National Polytechnic School, ENP, Algiers, Algeria.*
[2] *Research Laboratory in Electrical Engineering and Automatic (LREA), Medea, Algeria.*

Received: May 13, 2015; Revised: January 27, 2016

Abstract: The purpose of this paper is to present an approach to control the nonlinear system represented here by permanent magnet synchronous machines with two forms of control. This approach results from a combination of the adaptive and predictive properties, and the interaction of continuous-time and discrete event systems. Such a hybrid system consists of a discrete program with an analog environment. Many of the control approaches are limited to discrete-time hybrid systems because many complex mathematical issues are removed. In many applications the command variables are intrinsically discrete, either because such a system design is simpler or for other technological reasons. Our system consists of a five level inverter which controls a synchronous permanent magnet machine by predictive adaptive control, also, multilevel inverter is an effective solution for increasing power and reducing harmonics of AC waveforms.

Keywords: *PMSM-GPC; adaptive predictive control; structure cascade hybrid inverter.*

Mathematics Subject Classification (2010): 93C40, 34A38.

* Corresponding author: mailto:h_tlemcani@yahoo.fr

1 Introduction

The hybrid dynamic systems are systems that consist of coupled discrete and continuous components. Any electromechanical system with computerized controller is a hybrid system in general. In the past, the modeling and analysis of hybrid system have been done separately for its discrete and continuous components. The overall system is designed in a rather empirical fashion. Since computer-aided control is becoming more and more significant in modern system design practice, we face a major challenge: the development of intelligent, reliable, robust and safe computer-controlled systems [1–4]. The foundation for modeling and analysis systems must be established formatting [5].

Whatever be the electro-mechanical system it has be ruled by the following equation

$$[S] = [P] * [A] * [C], \tag{1}$$

where: S is an electro-mechanical system, P is a power supply, A is an actuator, C is a control. Hence, to make the system working at its optimum and running under the most efficient ability the parameters of the equations have to meet the following criteria:

$$[S]_r = [P]_p * [A]_s * [C]_o. \tag{2}$$

So, to construct a system that works in optimal status and in very favorable conditions, i.e. that tends towards to ideal, we must construct a highly reliable actuator with a good yield, good stability, and with a perfect power supply and robust control.

We need to add the third term so that the system operates in a closed loop. We explain the three terms of equation (2).

2 Electro-Mechanical System

Our actuator [A] is synchronous permanent magnet motor (PMSM), which has good characteristics such as high power density, high torque to inertia ratio and efficiency, The use of permanent magnet synchronous machine (PMSM) is in constant progress, in particular in the areas where significant performance is needed. The specific contributions of the synchronous machine are in relation to the gain in weight and volume, but also in the dynamic, thanks to more efficient control laws. For these reasons, this type of actuator is strongly preferred in the field of aeronautics [6, 7].

2.1 Machine model PMSM

The equations of electrical machines are described in reference d, q by the following equations [8]:

$$\begin{aligned}
\frac{di_d}{dt} &= -\frac{R}{Ld} i_d + \frac{L_q}{L_d} p\ \Omega\ i_q + \frac{1}{L_d} v_d, \\
\frac{di_q}{dt} &= -\frac{R}{L_q} i_q + \frac{L_d}{L_q} p\ \Omega\ i_d - \frac{\phi_f}{L_q} p\ \Omega + \frac{1}{L_q} v_q, \\
\frac{d\Omega}{dt} &= \frac{3p}{2J}(\phi_f i_q + (L_d - L_q) i_d i_q) - \frac{1}{J} T_r - \frac{F_c}{J} \Omega,
\end{aligned} \tag{3}$$

where v_d, v_q, i_d, i_q represent the stator voltages and currents returned to the axis d and q.

3 The Power Supply Study

The power supply is represented here by Multivel voltage-source inverters, that have been receiving more and more attention in the past few years for high- and medium-power induction-motor (IM) drive applications. Many multilevel inverter configurations and pulse width modulation (PWM) techniques are presented to improve the output voltage harmonic spectrum [9,10]. Some of the popular multilevel configurations are the neutral point clamped (NPC), series-connected H-bridge, flying capacitor, etc. Although they can be configured for more than two levels, as the number of levels increases, the power circuit and control complexity due to a large number of devices, increase. An optimum topology for multilevel inverters with more than three levels has not been achieved until now [9,11,12].

A multilevel inverter has four main advantages over the conventional bipolar inverter. First, the voltage stress on each switch is decreased due to series connection of the switches. Therefore, the rated voltage and consequently the total power of the inverter could be safely increased. Second, the rate of change of voltage (dv/dt) is decreased due to the lower voltage swing of each switching cycle. Third, harmonic distortion is reduced due to more output levels. Forth, lower acoustic noise and electromagnetic interference (EMI) is obtained [13,14].

Furthermore, the proposed hybrid PDPWM offers better harmonic performance compared to its conventional PWM counterpart [9], applying this technique for supplying the PMSM.

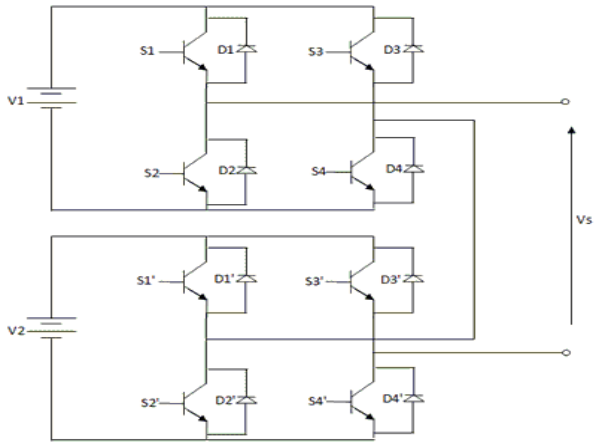

Figure 1: Schematic diagram of the inverter topology used to verify the proposed hybrid modulations.

Multilevel pulse width modulation is based on comparison of sinusoidal reference signal with each carrier to determine the voltage level that the inverter should switch to. Carrier based N level PWM operation consists of N-1 different carriers [13,15]. The carriers have the same frequency f_c, the same peak to peak amplitude V, and are disposed so that the bands they occupy are contiguous. They are defined as [13]

$$C_i = V\left((-1)^{f(i)}y_c(\omega_c,\varphi) + i - \frac{N}{2}\right), \quad i = 1,\ldots,N-1, \tag{4}$$

where y_c is a normalized symmetrical triangular carrier defined as

$$y_c(\omega_c, \varphi) = (-1)^{[\alpha]} ((\alpha \ mod \ 2) - 1) + \frac{1}{2}, \tag{5}$$

$$\alpha = \frac{\omega_c t + \varphi}{\pi}, \qquad \omega_c = 2\pi f_c, \tag{6}$$

where φ represents the phase angle of y_c, y_c is a periodic function with the period $T_c = 2\pi/\omega c$. It is shown that using symmetrical triangular carrier generates less harmonic distortion at the inverter's output [16].

While the multilevel PWM techniques developed thus far have been extensions of two level PWM methods, the multiple levels in a cascaded inverter offer extra degrees of freedom and greater possibilities in terms of device utilization, state redundancies, and effective switching frequency.

In this paper, we proposed this method [13]. The hybrid multilevel PWM scheme is presented which takes advantage of the special properties available in conventional PWM methods and minimizes switching losses with better harmonic performance. Figure 2 shows the carriers and the reference signals for a five level PWM using PD technique with $mi = 0.8$ and carrier frequency $f_c = 1050hz$ [13].

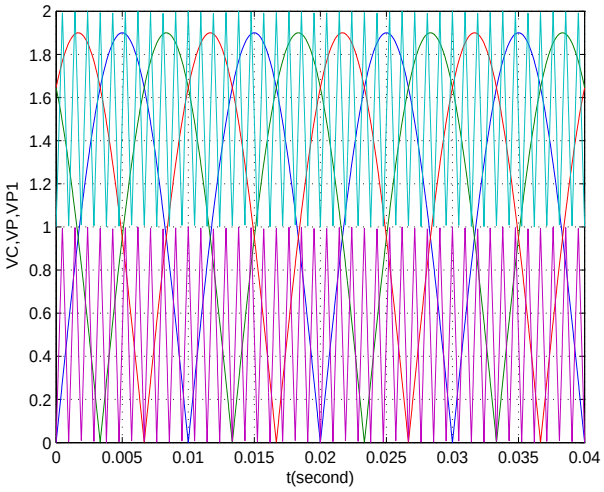

Figure 2: The references and carrier waves (triangular) for a five level inverter.

The proposed hybrid PWM is the combination of low frequency PWM and high frequency SPWM. In each cell of cascaded inverter, the four power devices are operated [13].

At two different frequencies, two being commutated at low frequency, i.e., the fundamental frequency of the output, while the other two power devices are pulse width modulated at high frequency. This arrangement causes the problem of differential switching losses among the switches [13].

An optimized sequential signal is added to the hybrid PWM pulses to overcome this problem. The low and high frequency PWM signals are shown in Figure 3. An optimized hybrid PDPWM method commutates the power switches at high frequency and

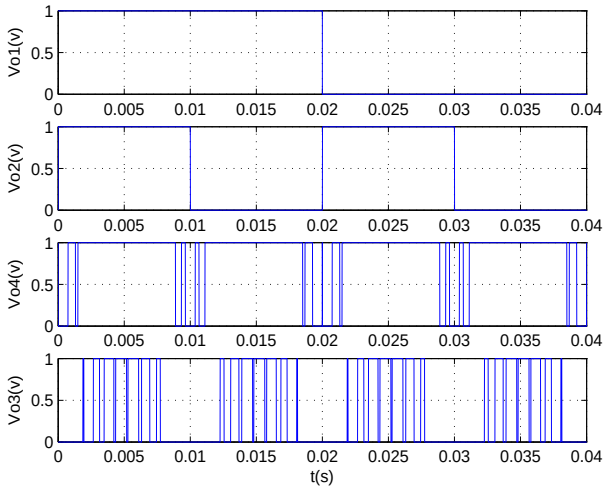

Figure 3: Low and high frequency hybrid PWM pulses at mi=0.8 and $f_c = 1050hz$.

low frequency sequentially. A common sequential signal and low frequency PWM signals are used for all cells in cascaded inverter. A high frequency SPWM for each cell is obtained by the comparison of the rectified modulation waveform with corresponding phase disposition carrier signal. The low frequency PWM signal should be synchronized with the modulation waveform. In Figure 4, the gate pulses are generated by a hybrid PWM controller. This controller is designed to mix the sequential signal, low frequency PWM and high frequency phase disposition sinusoidal PWM and to generate the appropriate gate pulses for cascaded inverter [17].

The previous section has presented the formulation of an optimized hybrid PDPWM switching pattern of a five level inverter. For completeness, the generalized formulation that suits N level inverter is presented [13].

4 Generalized Predictive Controller

The MPC provides various algorithms and the best algorithm is generalized predictive algorithm (GPC). MPC is one of the advanced control strategies, which can forecast the future response of the plant and optimize the control input with the help of a model of the plant. The prediction model will be augmented by the model of state space matrices [18].

In recent years, model predictive control (MPC) seems to be one of the most attractive advanced process control algorithms both in academia and in industry. The combination of new control design concepts in MPC, such as model prediction, receding horizon optimization and real-time correction, makes it possible to yield high performance for control systems. Among various MPC algorithms, general predictive control (GPC) has received particular attention. However, in contrast to the rapid development of MPC in application areas, the theoretical study of MPC properties seems still scarce. Only a little number of studies have been focused on the closed-loop properties of GPC and other MPC algorithms in relationship with the tuning parameters. Among these, excellent results

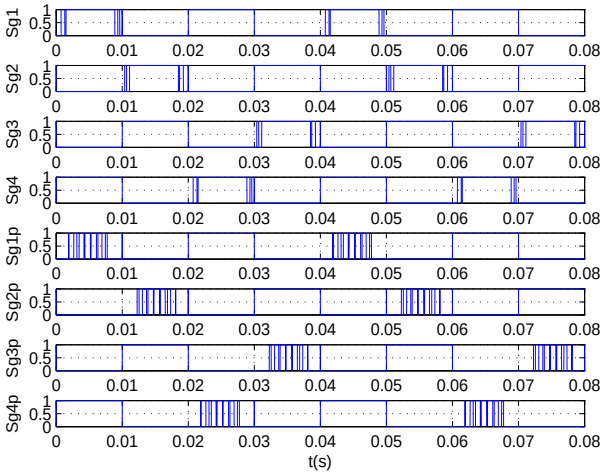

Figure 4: Optimized hybrid PWM switching pattern for five level cascaded multilevel inverter.

have been achieved by Clarke et al [19,20]. In the form of LQ problem, some new results on the GPC properties such as deadbeat control and stability were presented [19].

4.1 Formulation of Generalized Predictive Control

Most single-input single-output (SISO) plants, when considering operation around particular set points and after linearization, can be described by equation (7) [21].

$$A(q^{-1})y(t) = B(q^{-1})u(t) + C(q^{-1})\xi(t), \tag{7}$$

where $u(t)$ and $y(t)$ are the control and output sequence of the plant and $\xi(t)$ is a zero mean white noise. A, B and C are the following polynomials in the backward shift operator q^{-1}:

$$\begin{aligned} A(q^{-1}) &= 1 + a_1 q^{-1} + \cdots + a_{na} q^{-na}, \\ B(q^{-1}) &= q^{-d}\left(b_0 + b_1 q^{-1} + \cdots + b_{nb} q^{-nb}\right), \\ C(q^{-1}) &= 1 + c_1 q^{-1} + \cdots + c_{na} q^{-na}, \end{aligned} \tag{8}$$

where d is the dead time of the system. This model is known as a controller auto-regressive moving-average (CARIMA) model. It has been argued that for many industrial applications in which disturbances are non-stationary an integrated CARMA (CARIMA) model is more appropriate. A CARIMA model is given by equation (9) [21]:

$$A(q^{-1})y(t) = B(q^{-1})u(t) + C(q^{-1})\frac{\xi(t)}{\Delta(q^{-1})} \tag{9}$$

with $\Delta(q^{-1}) = 1 - q^{-1}$. For simplicity, polynomial C in equation (9) is chosen to be 1. Notice that if C^{-1} can be truncated it can be absorbed into A and B.

From the previous equation (9), a polynomial optimal predictor is designed in the following form:

$$y(t+j) = [F_j(q^{-1})y(t) + H_j(q^{-1})\Delta u(t-1)] + [G_j(q^{-1})\Delta u(t+1) + J_j(q^{-1})\xi(t+j)], \quad (10)$$

where G_j, F_j, H_j, J_j are the terms representing respectively the future, present, past, and the term related to disturbance. The first bracketed expression in equation (10) represents the free response. The criterion is a weighted sum of square predicted future errors and square control signal increments.

Cost Function

GPC algorithm consists of applying a control sequence that minimizes a cost function of the form given in equation (11) [21]:

$$j = \sum_{N_1}^{N_2} \left(\hat{y}(t+j) - w(t+j)\right)^2 + \lambda \sum_{N_1}^{N_u} \Delta u(t+j-1)^2. \quad (11)$$

Under the hypothesis

$$\Delta u(t+j) = 0 \quad \forall j \geqslant N_u \quad (12)$$

with: $w(t+j)$ reference applied at time $t+j$, $\hat{y}(t+j)$ predicted output at time $t+d$, $u(t+j-1)$ command increment at the instant $t+j-1$.

The relation (12) indicates that when the step of prediction j reaches the value fixed for the control horizon N_u, the change order will be canceled and therefore the future order will stabilize. This hypothesis will eventually simplify the control calculation.

The criterion requires the definition of four setting parameters, where N_u is the control horizon, N_1 is the minimum prediction horizon, N_2 is the maximum prediction horizon and λ are control weighting factors.

The control law is obtained by minimizing the previous criterion $\dfrac{\partial J}{\partial u} = 0$ such as

$$\widetilde{U} = M[w - \mathrm{if}(q^{-1})y(t) - \mathrm{ih}(q^{-1})\Delta u(t-1)]. \quad (13)$$

By reason of certain benefits introduced by the polynomial structure, we chose to formulate the control law in the canonical form of an RST controller.

Conventionally, in predictive control, only the first value of the sequence, equation (13) is finally applied to the system in agreement with the strategy of receding horizon, the whole process being effected again at the period of next sampling

$$\Delta u_{opt}(t) = -m_1' \left[\mathrm{if}(q^{-1})y(t) + \mathrm{ih}(q^{-1})\Delta u(t-1) - w\right] \quad (14)$$

with m_1': first row of the matrix M.

The GPC controller is implemented in a form of the RST by difference equation:

$$S(q^{-1})\Delta(q^{-1})u(t) = -R(q^{-1})y(t) + T(q)w(t). \quad (15)$$

This provides by identification the three polynomials R, S and T constituting the equivalent linear regulator [18]:

$$\begin{aligned} S(q^{-1}) &= 1 + m_1'\mathrm{ih}(q^{-1})q^{-1}, & d^\circ\left[S(q^{-1})\right] &= d^\circ\left[B(q^{-1})\right], \\ R(q^{-1}) &= m_1'\mathrm{if}(q^{-1})q^{-1}, & d^\circ\left[R(q^{-1})\right] &= d^\circ\left[A(q^{-1})\right], \\ T(q) &= m_1'\left[q^{N_1} \ldots q^{N_2}\right]', & d^\circ\left[T(q)\right] &= N_2, \end{aligned} \quad (16)$$

with:

$$\begin{aligned} \mathrm{if}(q^{-1}) &= \left[F_{N_1}(q^{-1}) \dots F_{N_2}(q^{-1})\right]', \\ \mathrm{ih}(q^{-1}) &= \left[H_{N_1}(q^{-1}) \dots H_{N_2}(q^{-1})\right]', \\ \widetilde{U} &= \left[\Delta u(t) \dots \Delta u(t+N_u-1)\right]', \\ \hat{y} &= \left[\hat{y}(t+N_1) \dots \hat{y}(t+N_2)\right]', \\ w &= \left[w(t+N_1) \dots w(t+N_2)\right]' \end{aligned} \tag{17}$$

$$G = \begin{bmatrix} g_{N_1}^{N_1} & g_{N_1-1}^{N_1} & \cdots & \cdots \\ g_{N_1+1}^{N_1+1} & g_{N_1}^{N_1+1} & \cdots & \cdots \\ \cdots & \cdots & \cdots & \cdots \\ g_{N_2}^{N_2} & g_{N_2-1}^{N_2} & \cdots & g_{N_2-N_u+1}^{N_2} \end{bmatrix}.$$

4.2 Reformulation of GPC control with adaptive control

We start with the definition of the performance error. Consider first the following regressor [22]. The starting point of this reformulation is constituted of setting equation presented in the previous paragraph, in particular, relationships to obtain the optimal control sequence.

4.3 Vectors parameters and regressor

The control law equation (13) may be transcribed in the form of the following matrix:

$$Mw = \theta' \Phi(t) \tag{18}$$

which involves the matrix of parameters θ of dimension $(n_a + n_b + N_u + 1) \times N_u$ with n_a and n_b being degrees of $A(q^{-1})$ and $B(q^{-1})$, respectively,

$$\theta' = [M\mathrm{if} \quad |_{Nu} \quad M\mathrm{ih}], \tag{19}$$

where if and ih matrices are formed of polynomial coefficients contained in $\mathrm{if}(q^{-1})$ and $\mathrm{ih}(q^{-1})$, and the following vector called regressor dimension $(n_a + n_b + N_u + 1)$:

$$\Phi(t) = \left[y(t) \dots y(t-n_a) \quad \widetilde{u}' \quad \Delta u(t-1) \dots \Delta u(t+n_b)\right]. \tag{20}$$

The matrix of parameters θ contains, on its first line, the coefficients of the polynomials R and S'. Indeed, from equation (14), the polynomial $m_1' \mathrm{if}(q^{-1})$ corresponds to R and $m_1' \mathrm{ih}(q^{-1}) q^{-1}$ corresponds to S'. The regressor $\Phi(t)$ is the output vector and past orders including unknown commands $\widetilde{u}$ of dimension N_u.

We also note that when $N_u = 1$, the matrix θ is reduced to a vector including direct polynomial coefficients R and S'.

4.4 The method for updating

The matrix controller parameters can be updated as most of strategies. Here we can mention the gradient method and the recursive least squares method

$$\hat{\theta}(t+1) = \hat{\theta}(t) + F\phi(t)\varepsilon^0(t+1) \tag{21}$$

with the use of the algorithm of Trace constant for determining the adaptation gain at time t. To obtain a recursive algorithm, we consider the estimate $\hat{\theta}(t+1)$.

After development, it follows the A.A.P:

$$\hat{\theta}(t+1) = \hat{\theta}(t) + F(t+1)\phi(t)\varepsilon^0(t+1) \tag{22}$$

with

$$F(t+1) = F(t) - \frac{F(t)\phi(t)\phi(t)^T F(t)}{1+\phi(t)^T F(t)\phi(t)}, \tag{23}$$

where $\hat{\theta}$ is the vector of the estimated parameters and $F(t+1)\phi(t)\varepsilon^0(t+1)$ represents the correction term, F is the adaptation gain, ϕ is the vector of observations (or measures) and ε is the prediction error (error adaptation), that is to say the difference between the measured process output and the predicted output [22].

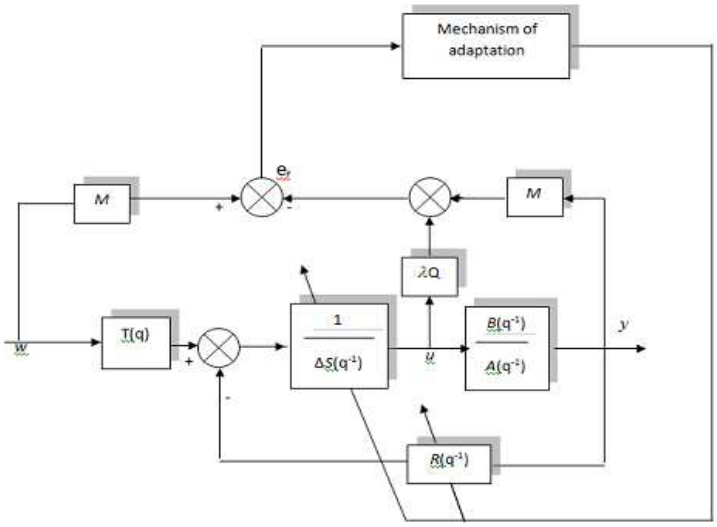

Figure 5: Structure equivalent of direct adaptive predictive control, control loop of RST and adaptation mechanism.

5 Simulation Results and Discussion

Figure 6 represents the overall structure of speed control of PMSM fed by a hybrid structure cascade five-level inverter, using the adaptive predictive control. To test the effectiveness of the proposed control strategy for adjusting the speed, we have used numerical simulation in the following cases:

- Step response of speed.
- Start unloading and then applying a torque resistant.
- Reverse speed.

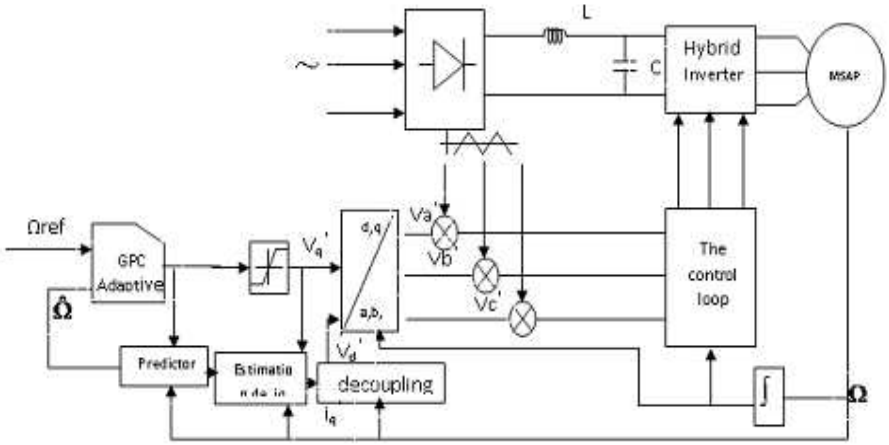

Figure 6: Global structure for regulating the PMSM.

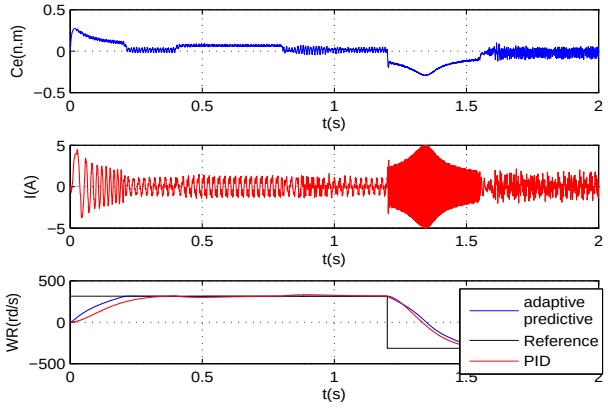

Figure 7: PMSM performance of the machine fed by the hybrid inverter.

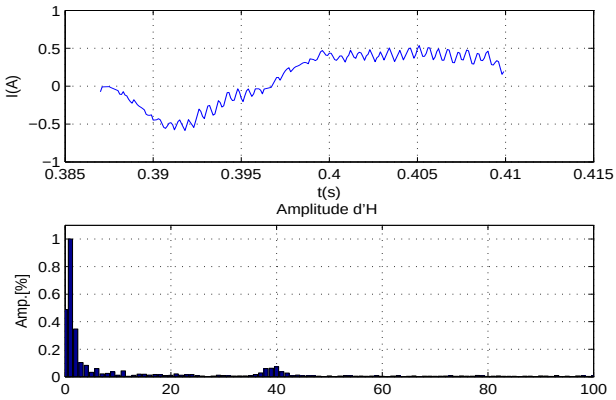

Figure 8: Top trace is phase current (ia). Second trace is normalized harmonic spectrum of phase current (technique of PI controller fed by five level inverter (NPC)).

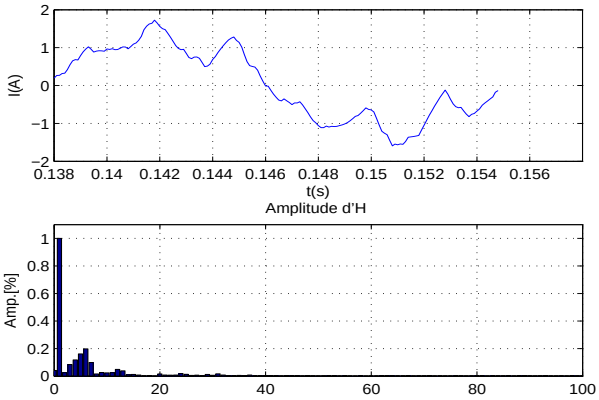

Figure 9: Top trace is phase current (ia). Second trace is normalized harmonic spectrum of phase current (technique of adaptive predictive control fed by five level inverter (NPC)).

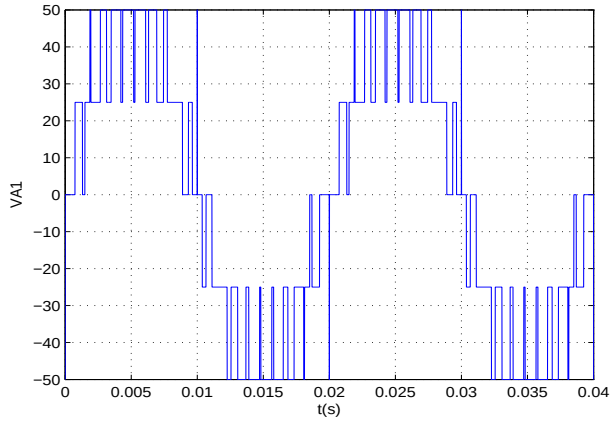

Figure 10: Output phase voltage waveform.

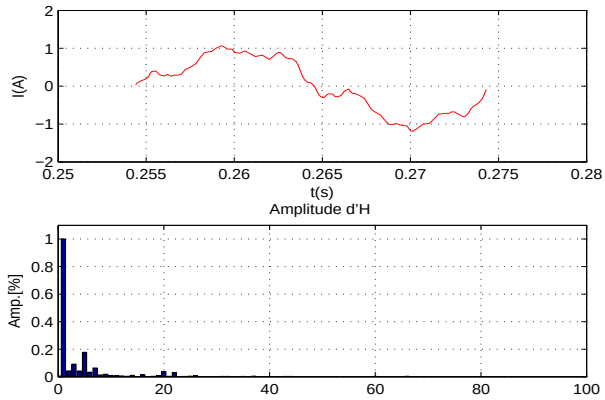

Figure 11: Top trace is phase current (ia). Second trace is normalized harmonic spectrum of phase current (technique of adaptive predictive control fed by hybrid inverter).

Table 1. Comparison of different strategies proposed.

Controller With power supply	PI with five livel (NPC)	adaptive Predictive with five livel(NPC)	adaptive Predictive with hybrid inverter.
Rotor speed	314(rd/s) at 0.4sec	314(rd/s) at 0.2 sec	314(rd/s) at 0.2 sec
THD	37.95	30.85	22.41

5.1 Discussion of the results of adaptive predictive control

As shown in Figure 7 it appears that for a reference of 314 rd/s during unloaded starting, the steady state is achieved at $t = 0.2s$, which is a very appreciable response time, compared with the conventional PID controller. The application of the load between $t = 0.4s$ and $0.8s$ causes a slight loss of speed that is quickly restored. Also note that this load has no influence on the direct current component, indicating that the vector control is effective. By analyzing the graph of the harmonic spectrum of the phase current, we notice that there is a very big improvement in the pace of the phase current compared to a five-level inverter. Finally, when reversing the speed reference we observe an excessive increase in the starting current, which is justified by the large variation subjected to the machine (from 314rd /s to -314rd /s). The time of the establishment of the speed increased slightly to reach $t = 0.34s$. However, upon reversal of the reference, we see an appearance of exceeding in terms of the response, so a runaway effect occurs, which led us to introduce an anti-windup device. The latter is not enough to limit the speed so it is recommended to act on the GPC parameters to remedy this problem.

5.2 Influence of the GPC parameters

As mentioned in references [23], for maintaining N_1, N_u, and λ_{opt} to the values 1, 1 and trace (G'G) respectively, and varying N_2 to reconcile between a rapid response and an acceptable startup current, it is necessary to find a set of parameters that can meet these requirements. To do this, the influence of parameters on the magnitudes of the PMSM is analyzed through the following figure: It appears that a strong increase for N_2 results

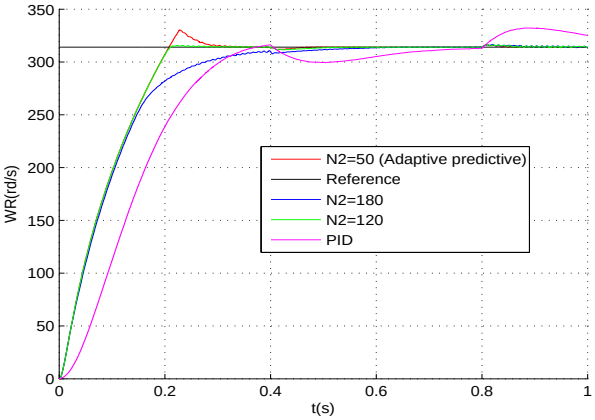

Figure 12: Parameter sets.

in a slow system response, while too large a decrease results in a large overshoot about the set-point (runaway). Note that when N_2 increases the response time increases. This leads to a supplementary computation time which, to be reduced, must be accompanied by an anti-windup device used primarily to limit both the speed around the set-point and the admissible starting current, in our case the best choice for N_2 or $N_{2_{optimum}} = 120$. It is clear that the time to response is very large in the case of conventional PID controller even if $N_2 = 180$, as well as the rejection of disturbance is very good in the adaptive predictive control (see Figure 12).

Also, the right choice of N_2 does not influence the response time only, but also the shape of the phase current. The following table clearly shows the THD of each value of N_2.

Table 2. Comparison of the THD for different values of N_2:

N_2:maximum prediction horizon	180	120	50
THD	31.78	22.41	48.75

6 Conclusion

The association between predictive control that has the ability to anticipate future events and can take control actions accordingly and the adaptive control whose main role is to eliminate the effect of disturbances in order to control better the system, relatively to the conventional controller. In addition, the proposed hybrid inverter gives better harmonic performance compared to its conventional homologue PWM. The simulation results show a vast improvement in the current waves and good agreement with the adaptive predictive control used to control the PMSM. Despite the introduction of the load and the inversion of the set-point, this system is characterized by a better control of the MASP transient regime, which conducts to good response times with an assured decoupling and a fast enough dynamic rejection of disturbances. With a good choice of the actuator (PMSM) and a robust control (adaptive predictive) and with a good fed (hybrid inverter) like

ours, we could check the first formula of our paper. Therefore our system can provide superior performances in terms of increased efficiency and reduced noise.

References

[1] Tlemçani, A., Sebaa, K. and Henini, N. Indirect adaptive fuzzy control of multivariable nonlinear systems class with unknown parameters. *Nonlinear Dynamics and Systems Theory* **14** (2) (2014) 162–174.

[2] Hamidia, F., Larabi, A., Tlemçani, A. and Boucherit, M. S. AIDTC Techniques for Induction Motors. *Nonlinear Dynamics and Systems Theory* **13** (2) (2013) 147–156.

[3] Henini, N., Nezli, L., Tlemçani, A. and Mahmoudi, M. O. Improved Multimachine Multiphase Electric Vehicle Drive System Based on New SVPWM Strategy and Sliding Mode - Direct Torque Control. *Nonlinear Dynamics and Systems Theory* **11** (4) (2011) 425–438.

[4] Benmansour, K., Tlemçani, A., Djemai, M. and De Leon, J. A New Interconnected Observer Design in Power Converter: Theory and Experimentation. *Nonlinear Dynamics and Systems Theory* **10** (3) (2010) 211–224.

[5] Zhang, Y. and Mackworth, K. *Logical Foundations for Cognitive Agents* (1999) 370–396.

[6] Fadel, M. and Linh Nguyen, N. Different Solutions of Predictive Control for tow Synchronous Machines in Parallel. In: *International symposium on IEEE* (2013) 1–7.

[7] Louis, J.P. *Control of Synchronous Motors.* London, Wiley-ISTE, 2011.

[8] Nguyen, D. Dutta, R. and Rahman, M. F. Investigating characteristics of a concentrated-winding interior permanent magnet synchronous machine for sensorless direct torque control. In: *International Symposium on IEEE*, 2013.

[9] Sivakumar, K. Ramchand, R. and Gopakumar, K. A Hybrid Multilevel Inverter Topology for an Open-End Winding Induction-Motor Drive Using Two-Level Inverters in Series With a Capacitor-Fed H-Bridge Cell. *IEEE transactions on industrial electronics* **57** (11) (2010) 3707–3714.

[10] Rodriguez, J., Bernet, S., Wu, B., Pontt, J.O. and Kouro, S. Multilevel voltage-source-converter topologies for industrial medium-voltage drives. *IEEE Trans. Ind. Electron.* **54** (6) (2007) 2930–2945.

[11] Busquets-Monge, S. Ortega, J. D. Bordonau, J. Beristain, J. A. and Rocabert, J. Closed-loop control of a three-phase neutral-point-clamped inverter using an optimized virtual-vector-based pulse width modulation. *IEEE Trans. Ind. Electron.* **55** (5) (2008) 2061–2071.

[12] Nabae, A. Takahashi, I. and Agaki, H. A new neutral point-clamped PWM inverter. *IEEE Trans. Ind. Appl.* **IA-17** (5) (1981) 518–523.

[13] Govindaraju, C. and Baskaran, K. Optimized Hybrid Phase Disposition PWM Control Method for Multilevel Inverter. *International Journal of Recent Trends in Engineering* **1** (3) (2010) p. 36–40.

[14] Rodriguez, J., Lai, J.S. and Peng, F.Z. multilevel inverter: Asurvey of topologies, controls and applications. *IEEE Trans. Ind. Electron.* **49** (4) (2002) 724–738.

[15] Mcgrath, B.P. and Holmes, D.G. Multicarrier PWM strategies for multilevel inverters. *IEEE Trans.Ind.Electron.* **49** (4) (2002) 858–867.

[16] Hamman, J. and Van Der Merwe, F.S. Voltage harmonics generated by voltage fed inverters using PWM natural sampling. *IEEE Trans. Power Electron* **PE-3** (3) (1988) 297–302.

[17] Hema Maheshwari, V. Soundradevi, G. Karthikeyan, B. and Sundari, G. A 11 level cascaded multilevel inverter using hybrid modulation technique. *International Journal of Emerging Trends in Engineering and Development* **2** (2013).

[18] Manimaran, M., Arumugam, A. and Ramkumar, K. Parameter Estimation based Optimal control for a Bubble Cap Distillation Column. *International Journal of Chem Tech Research IJCRGG* **6** (1) (2014) 790–799.

[19] Zhang, J. and Xi, Y. *Study on the Closed-loop Properties of GPC.* Chinese National Science Foundation (1991) 1–13.

[20] Clarke, D.W. and Mohtadi, C. Property of Generalized Predictive Control. *Automatica* **25** (6) (1989) 859–875.

[21] Chidrawar, S. and Patre, B. Generalized Predictive Control and Neural Generalized Predictive Control. *Leonardo Journal of Sciences* **13** (2008) 133–152.

[22] Dumur, D. Contribution L'analyse et au Développement D'algorithmes de Commande Prédictive, Rapport de Synthese (Habilitation à diriger des recherches), Universite Paris XI, 2002.

[23] Dumur, D. and Boucher, P. A review introduction to linear GPC and applications. *Journal A* **39** (4) (1998) 21–35.